CHINESE OPTICS LETTERS

Vol. 19, No. 1 | January 2021

Effect of purification, dehydration, and coagulation processes on the optical parameters of biological tissues

Halil Arslan* and Bahar Pehlivanoz

Faculty of Technology, Electrical and Electronics Engineering Department, Sakarya University of Applied Sciences, Sakarya, Turkey

*Corresponding author: harslan@sakarya.edu.tr

Received July 2, 2020 | Accepted August 28, 2020 | Posted Online November 24, 2020

In this study, the effects of purification, dehydration, and coagulation processes on the absorption and reduced scattering coefficients of chicken liver tissues have been investigated by using a single integrating sphere system. The purification process performed on the tissue samples to remove blood residue has been found to cause a slight change in the optical parameters. Although the dehydration process brings about an increase in the absorption coefficient due to the water loss, no direct relationship has been observed between the reduced scattering coefficient and the dehydration level of the tissue. In addition, it has been observed that there was a relatively small increase in the absorption coefficient and a significant increase in the reduced scattering coefficient after the coagulation process. Therefore, it can be said that the optical penetration depth decreased significantly after dehydration and coagulation processes unlike blood purification. Moreover, fluence rate distributions inside the fresh, blood purified, dehydrated, and coagulated tissue models have been investigated by using the Monte Carlo modeling of photon transport in multilayered tissues simulation code.

Keywords: optical properties; dehydration; coagulation; integrating sphere; IAD.
DOI: 10.3788/COL202119.011701

1. Introduction

Light has been clinically used in the diagnosis and treatment of various diseases for many years. The use of light in medical applications has increased, especially with the development of lasers, optical fibers, and optical detectors. Therefore, it has become important to calculate the optimum dose of light to be applied and understand the light–tissue interaction in order to make an accurate diagnosis or to perform a successful treatment. In this context, the knowledge of light propagation in the target tissue, which has been identified with optical parameters of tissue, is needed[1].

While light travels in the tissue, it can be absorbed, scattered, or transmitted depending on not only the wavelength of the light, but also the optical properties of the tissue. Absorption is directly related to oxygen saturation, as well as the concentration of chromophores in the tissue such as hemoglobin, water, and melanin. Scattering gives information about lipid concentration, cell nucleus size, and change of cell membrane refractive index[2]. Light propagation inside biological tissue is characterized by the absorption coefficient, scattering coefficient, and anisotropy factor, which are the main optical parameters of tissues. The absorption coefficient (μ_a) is a measure of the probability of light absorption within tissue of a unit length. Similarly, the scattering coefficient (μ_s) describes the probability of unit length scattering. In addition, the anisotropy factor (g) is the mean cosine of the deflection angle due to scattering of the photon. Moreover, the reduced scattering coefficient (μ_s'), which is a parameter that fully reflects the scattering feature in media, has been defined in terms of the anisotropy factor and the scattering coefficient with the equation of

$$\mu_s' = \mu_s(1-g). \tag{1}$$

Light propagation in a medium can be described mathematically by using two different theories, which are analytical theory and transport theory. Analytical theory, which is in principle the most basic approach, is based on the physics of Maxwell's equations. However, its applicability is limited due to the complexities of the analytical solutions. Transport theory is defined by the radiative transport equation (RTE), and it is based on the principle of transporting photons from a medium (such as biological tissues) containing randomly distributed scattering and absorbing particles. Compared to Maxwell's equations, RTE has been used more widely in order to define the light propagation inside the biological tissues[3].

Many experimental methods and theoretical models have been used to obtain optical parameters of tissue from total diffuse reflection and total diffuse transmission values based on the RTE solution. The most commonly used techniques or models

are Monte-Carlo simulation[4,5], inverse adding doubling (IAD)[6,7], Beer–Lambert law[8], integrating sphere system[9,10], Kubelka–Munk model[11,12], inverse Monte-Carlo simulation[13], and diffusion approximation[14,15].

Diagnosis and treatment applications differ in the interaction type of the light with target tissue. There are mainly five types of interactions, which are photo-chemical interactions, thermal interactions, photo-ablation, plasma-induced ablation, and photo-disruption[16]. Such interactions are heavily dependent on the physical and chemical properties of biological tissues together with the wavelength, optical power, and exposure time. For example, laser-induced interstitial thermotherapy (LITT), in which photo-thermal interaction is important, has been formed as a basis of a new tumor treatment technique with the possibility of tissue coagulation[17]. In addition, various procedures are needed to be applied on tissue samples in some experimental studies. For example, tissues can be kept in isotonic saline solution to prevent water loss before the measurements. Since all of these processes result in some changes in the optical properties of the tissues, it is important to determine how much these changes are crucial for not only laboratory studies but also medical applications.

In this study, the effects of various processes, which are blood purification, dehydration, and coagulation, on the optical parameters of biological tissue samples have been investigated. By using the experimental results, fluence rate distributions inside modelled tissues, which were exposed to these processes, have been obtained with the help of Monte Carlo simulations.

2. Materials and Methods

In this study, a single integrating system has been used to determine the optical parameters of the prepared tissue samples. A schematic view of the experimental setup is illustrated in Fig. 1.

The photodynamic therapy (PDT) laser device used in the experiment can operate up to a maximum of 1.5 W optical power at a fixed 635 nm wavelength. The wavelength spectrum of the device is given in Fig. 2. The device, detailed information about which can be found in Ref. [18], was designed for use together with the photo-sensitizers that have relatively higher absorption around 635 nm. For example, 5-aminolevulinic acid (5-ALA) is medically used effectively together with 635 nm light sources[19,20].

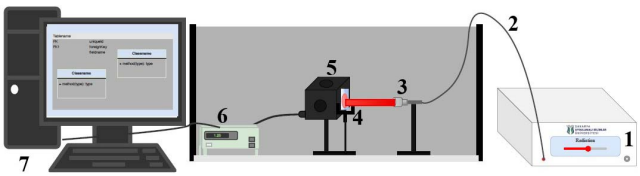

Fig. 1. Schematic view of experimental setup. 1, PDT laser device; 2, fiber optics cable; 3, collimator; 4, tissue samples; 5, integrating sphere; 6, photodiode amplifier; 7, computer.

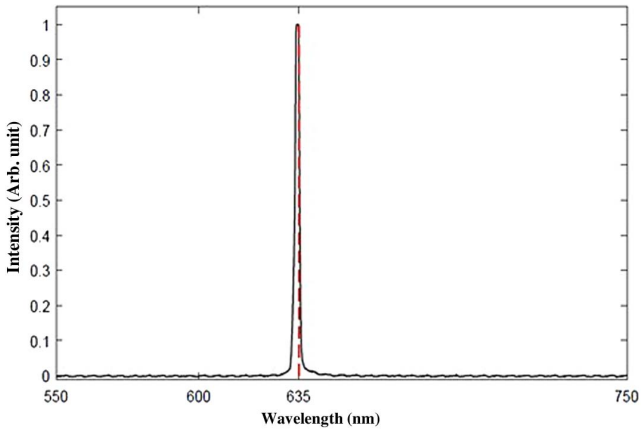

Fig. 2. Wavelength spectrum of the PDT laser device.

Chicken liver tissue has been used in the experiments. Tissues have been cut into flat sheets of port size of the integrating sphere and sandwiched between two microscope slides. Prepared tissue samples have been divided into four different groups, each of which has been exposed to different experiment conditions.

The first experimental group has been formed with fresh tissue samples that have the thickness between 0.8 mm and 1 mm. Since the loss of the freshness causes change in the optical parameters of the tissues[21], freshness of the tissues used in the experiments has been taken care of.

For the second group, tissue samples have been kept in 0.9% isotonic saline solution for 10 min. Then, the samples have been removed from the solution and waited for 2–3 min before they are placed between two slides. Tissue thicknesses have been measured with a micrometer and recorded for later use.

Considering that the water concentration in the tissue affects the optical parameters, the third experiment group has been prepared to investigate the effect of dehydration. This group has been divided into two subgroups named dehydration and control. Samples belonging to the control group have been fixed between the two microscope slides. On the other hand, the samples of the dehydration group have been placed on a single glass slide. The thicknesses and the weights of the tissue samples in each subgroup have been measured before they are placed in a 37°C electro-thermal incubator. Tissue samples, which were kept in the incubator for different durations (4, 8, 12, 16, 20, 24 h), have been removed from the incubator, and their thicknesses and weights have been measured again. Dehydration level for each tissue sample has been calculated by using the equation of

$$\omega = \frac{m_f - m_d}{m_f}, \tag{2}$$

where m_f and m_d are the weights of fresh and dehydrated samples, respectively. In order to reduce the statistical uncertainty, nine samples have been prepared for each subgroup and period of time. The samples removed from the incubator have not been used again.

The fourth experimental group has been prepared to investigate the effect of coagulation. In this experimental group, tissue

samples have been kept in a 95°C water bath for 10 min. Finally, tissue samples have waited at room temperature for 5 min in order to ensure thermal equilibrium, and then coagulated tissue samples have been placed on two microscope slides to measure optical parameters.

A single integrating sphere system has been used for measurements of the total reflectance and the total transmittance values for all of the tissue samples. The values obtained from the measurements have been added to the data file in IAD software developed by Prahl[22]. IAD is an iterative program used to compute optical parameters by solving the transport equation. Optical parameters of the samples of each group have been expressed as the mean ± standard deviation (SD). The mean value has been obtained by performing three measurements for each tissue sample, and then the mean ± SD values have been calculated from different samples.

In addition, by using the Monte Carlo modeling of photon transport in multilayered tissues (MCML) code, chicken liver tissue samples have been modeled to have simple cylindrical geometries. The absorption and reduced scattering coefficient values obtained in the experimental part of the study have been used as input parameters of the simulations. The other input parameters, anisotropy factor and refractive index, have been determined on the basis of literature values for chicken liver tissue and taken as 0.9 and 1.37, respectively[23].

3. Results and Discussion

The absorption coefficient and reduced scattering coefficient of fresh chicken liver tissue for 635 nm have been determined to be $0.20 \pm 0.04\,\mathrm{mm}^{-1}$ and $0.94 \pm 0.09\,\mathrm{mm}^{-1}$, respectively. These values are quite compatible with the ones reported in the literature[24].

The purification process performed on the tissue is used during the sample preparation in order to remove blood residues. This method, which is also used for the storage of tissues, prevents the prepared tissue samples from drying out while waiting for the measurement. In some of the studies reported in the literature, tissue samples were stored in saline solution before the experiment[25,26]. Therefore, the second group of this study has been prepared in order to investigate the effect of saline solution on optical parameters. As the result of the measurements, absorption and reduced scattering coefficients of chicken liver tissue samples after blood purification have been determined to be $0.18 \pm 0.04\,\mathrm{mm}^{-1}$ and $0.98 \pm 0.05\,\mathrm{mm}^{-1}$, respectively. Compared to the fresh tissue, a small decrease in the absorption coefficient and a small increase in the reduced scattering coefficient have been observed. In other words, short-term storage of tissue samples in saline solution caused a slight change in the optical parameters.

The third group, consisting of two subgroups, has been prepared to estimate the effect of dehydration on optical parameters of the tissue samples. Dehydration levels of the tissue samples belonging to both dehydration and control groups are illustrated in Fig. 3 as a function of time.

At the end of 24 h, the maximum average weight loss has been found to be approximately 71% for the samples in dehydration group, while it was found to be 48% for the control group. The lower weight loss in the control group can be attributed to the second microscope slide, which covers the tissue sample and partially prevents the dehydration. In any case, depending on the dehydration level, both weights and thicknesses decrease with the loss of water. A sharp decrease in the hydration level during the first 12 h ensures that the weights of the tissue samples from both subgroups decrease with similar behavior. The weight loss gradually decreases as the samples are kept for longer times in the incubator.

Optical parameters of the tissue samples kept in the incubator are also affected due to dehydration. Absorption and reduced scattering coefficients of the tissue samples from the control and dehydration groups are given in Fig. 4 as a function of incubation time.

It can be seen from the figure that both absorption and reduced scattering coefficients of tissue samples increase with the incubation time. Therefore, it has become important to investigate the relationship between optical properties and dehydration level. The absorption and the reduced scattering coefficients are shown in Fig. 5 as a function of the dehydration level.

It can be obviously seen from the figure that the absorption coefficients of the tissue samples in both groups increase due to water loss in the tissue. Although the number of chromophores does not change[27], tissue samples shrink and density increases in the cells due to increased water loss. Hence, it can be said that there is a correlation between the absorption coefficient and dehydration level independent from how the sample is dehydrated. However, the reduced scattering coefficients of the samples from the dehydration group have been found to be almost the same for different dehydration levels. Furthermore, unlike the dehydration group, the reduced scattering coefficient of the control group increases with the increase in the dehydration level. Therefore, it can be concluded that there is no direct relationship between the reduced scattering coefficient and the dehydration level.

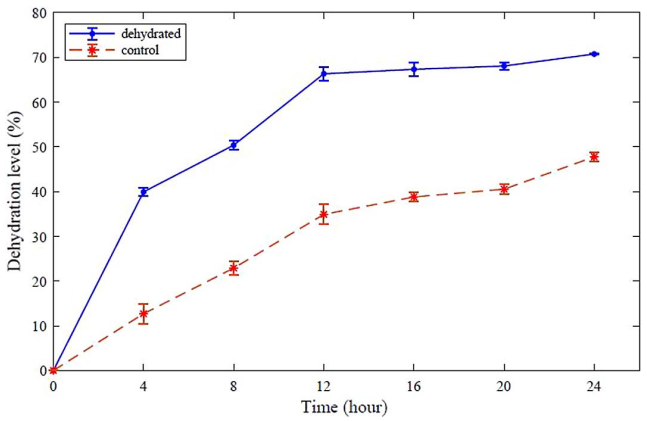

Fig. 3. Dehydration levels of the tissue samples as a function of time for dehydration and control groups.

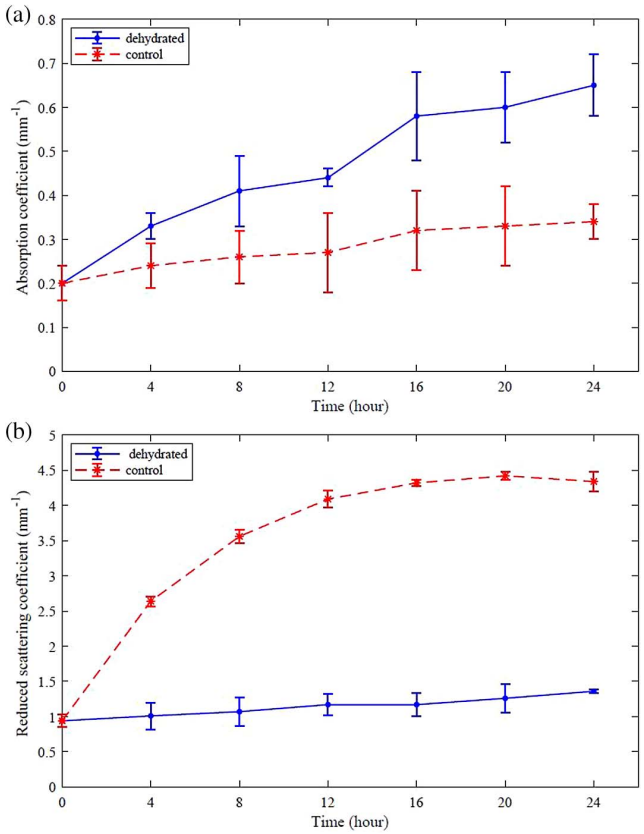

Fig. 4. (a) Absorption coefficient and (b) reduced scattering coefficient of the tissue samples as a function of incubation time.

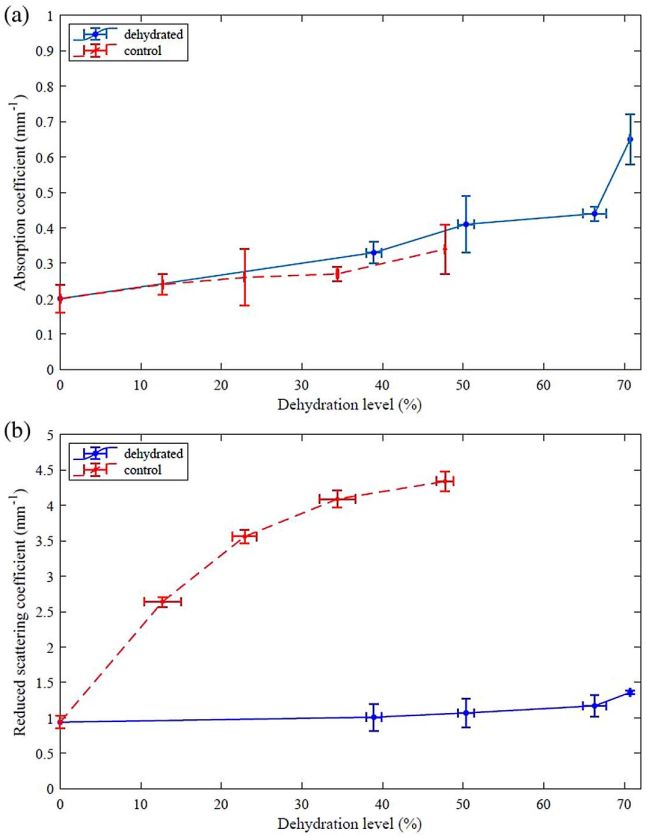

Fig. 5. (a) Absorption and (b) reduced scattering coefficients of tissue samples as a function of dehydration levels.

The last experimental group has been formed to examine the effects of coagulation on the optical parameters of chicken liver tissue. For this purpose, fresh tissue samples have been kept in a water bath set at 95°C. It has been observed that the appearances and structures of the tissue samples changed with the effect of the high temperature. It is known that the alterations in the structure and the appearance of tissues because of the photothermal processes result in the changes in the optical properties[28]. The absorption and reduced scattering coefficients of the coagulated tissue samples for 635 nm have been found to be $0.25 \pm 0.06\ \mathrm{mm}^{-1}$ and $9.28 \pm 0.92\ \mathrm{mm}^{-1}$, respectively. The liver tissue consists of scattering particles such as organelles, capillaries, cell nuclei, and cells that cause light scattering in tissues. Thermal coagulation brings about the changes in size, refractive index, and distribution of these particles. Consequently, increased incompatibility in the refractive indices results in an increase in the reduced scattering coefficient. It was previously reported that the increase in the absorption coefficient after thermal coagulation is due to the denser packing of cells owing to the shrinking of liver samples, with no change in the number of chromophores[29].

In addition to the experimental part, fluence rate distributions inside the fresh, blood purified, dehydrated, and coagulated tissue models have been investigated by using the MCML simulation code. MCML is one of the commonly used softwares for modeling light transport in heterogeneous and multilayer structures such as biological tissues[30]. The fluence rate distributions are given in Fig. 6 as a function of depth inside the tissue models. As can be expected, fluence rate distributions inside the fresh and purified tissue models have been obtained to be quite similar. Because of the relatively greater absorption or scattering coefficients, the distributions inside the dehydrated and coagulated tissue models have been found to be steeper. The increased absorption coefficient of dehydrated tissue causes a decrease in the number of photons at a certain depth. In addition, the

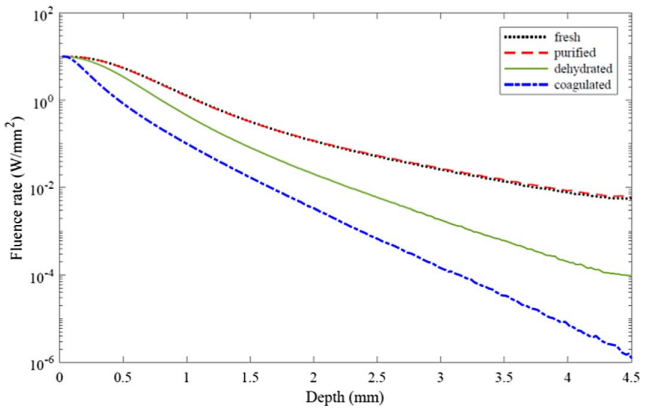

Fig. 6. Fluence rate distributions inside the fresh, purified, dehydrated, and coagulated tissue models as a function of depth.

reduced scattering coefficient of coagulated tissue indicates that multiple scattering occurs within the tissue. Therefore, the coagulation process causes a reduction in the optical penetration depth inside the biological tissues. Moreover, by looking at the distributions given in the figure, one can also conclude that optical penetration depth has the smallest value for the coagulated tissue model. The results of this study are in good agreement with similar studies performed by using different wavelengths of light and various types of tissue[21,27–33].

4. Conclusion

The processes, like purification, dehydration, and coagulation, could affect the blood, cell density, and water content inside the biological tissues. Because of this fact, the optical parameters and, accordingly, the fluence rate distributions inside the tissues are expected to be changed after such operations. In this study, the effects of purification, dehydration, and coagulation processes on the optical parameters of biological tissues have been investigated. For this purpose, absorption and reduced scattering coefficients of fresh, purified, dehydrated, and coagulated chicken liver tissue samples have been determined by using a single integrating sphere system.

It has been concluded that the purification process performed on the tissue samples to remove blood residues causes a very small decrease (increase) in the absorption (scattering) coefficient. In other words, short-term storage of tissue samples in saline solution causes a slight change in the optical parameters. In addition, the absorption coefficient of the samples increases after the dehydration process because of the water loss in the tissue. However, no direct relationship has been observed between the reduced scattering coefficient and the dehydration level. Moreover, the coagulation process causes an increase in not only the absorption coefficient but also the reduced scattering coefficient. Due to the increased incompatibility in refractive indices of scattering particles inside the tissue, an increase in the reduced scattering coefficient has been found to be relatively more pronounced.

Acknowledgement

This work was supported by the Scientific and Technological Research Council of Turkey, TUBITAK 3501 (Project No. 118E235).

References

1. S. L. Jacques, "Optical properties of biological tissues: a review," Phys. Med. Biol. **58**, R37 (2013).
2. V. Tuchin, *Tissue Optics: Light Scattering Methods and Instruments for Medical Diagnosis* (SPIE Press, 2007).
3. M. H. Niemz, *Laser-Tissue Interactions: Fundamentals and Applications* (Springer, 2007)
4. B. C. Wilson and G. Adam, "A Monte Carlo model for the absorption and flux distributions of light in tissue," Med. Phys. **10**, 824 (1983).
5. S. A. Prahl, M. Keijzer, S. L. Jacques, and A. J. Welch, "A Monte Carlo model of light propagation in tissue," SPIE Inst. Ser. **IS 5**, 102 (1989).
6. A. N. Bashkatov, E. A. Genina, V. I. Kochubey, and V. V. Tuchin, "Optical properties of human skin, subcutaneous and mucous tissues in the wavelength range from 400 to 2000 nm," J. Phys. D: Appl. Phys. **38**, 2543 (2005).
7. S. C. Gebhart, W. C. Lin, and A. Mahadevan-Jansen, "*In vitro* determination of normal and neoplastic human brain tissue optical properties using inverse adding-doubling," Phys. Med. Biol. **51**, 2011 (2006).
8. D. F. Swinehart, "The Beer–Lambert law," J. Chem. Educ. **39**, 333 (1962).
9. J. W. Pickering, S. A. Prahl, Niek van Wieringen, J. F. Beek, H. J. C. M. Sterenborg, and M. J. C. van Gemert, "Double-integrating-sphere system for measuring the optical properties of tissue," Appl. Opt. **32**, 399 (1993).
10. G. D. Vries, J. F. Beek, G. W. Lucassen, and M. J. C. V. Gemert, "The effect of light losses in double integrating spheres on optical properties estimation," IEEE J. Select. Top. Quantum Electron. **5**, 944 (1993).
11. P. Kubelka and F. Munk, "Ein Beitrag Zur Optik Der Farbanstriche," Zeitschrift für Technische Physik **12**, 593 (1931).
12. O. Hamdy, M. Fathy, T. A. Al-Saeed, J. El-Azab, and N. H. Solouma, "Estimation of optical parameters and fluence rate distribution in biological tissues via a single integrating sphere optical setup," Optik **140**, 1004 (2017).
13. G. M. Palmer and N. Ramanujam, "Monte Carlo-based inverse model for calculating tissue optical properties. Part I: theory and validation on synthetic phantoms," Appl. Opt. **45**, 1062 (2006).
14. J. L. Karagiannes, Z. Zhang, B. Grossweiner, and L. I. Grossweiner, "Applications of the 1-D diffusion approximation to the optics of tissues and tissue phantoms," Appl. Opt. **28**, 2311 (1989).
15. W. M. Star, J. P. A. Marijnissen, and M. J. C. van Gemert, "Light dosimetry in optical phantoms and in tissues. I. Multiple flux and transport theory," Phys. Med. Biol. **33**, 437 (1988).
16. N. Honda, T. Nanjo, K. Ishii, and K. Awazu, "Optical properties measurement of laser coagulated tissues with double integrating sphere and inverse Monte Carlo technique in the wavelength range from 350 to 2100 nm," Proc. SPIE **8221**, 82211F (2012).
17. C. T. Germer, A. Roggan, J. P. Ritz, C. Isbert, D. Albrecht, G. Müller, and H. J. Buhr, "Optical properties of native and coagulated human liver tissue and liver metastases in the near infrared rangelasers in surgery and medicine," Lasers Surg. Med. **23**, 194 (1998).
18. A. F. Kamanli, M. Z. Yildiz, H. Arslan, G. Çetinel, N. K. Lim, and H. S. Lim, "Development of a new multi-mode NIR laser system for photodynamic therapy," Opt. Laser Technol. **128**, 106229 (2020).
19. R.M. Szeimies, C. Abels, C. Fritsch, S. Karrer, P. Steinbach, W. Bäumler, G. Goerz, A.E. Goetz, and M. Landthaler, "Wavelength dependency of photodynamic effects after sensitization with 5-aminolevulinic acid in vitro and in vivo," J. Invest. Dermatol. **105**, 672 (1995).
20. H. Arslan and Y. B. Dolukan, "Optical penetration depths and fluence distributions in chicken breast and liver tissues," Opt. Spectrosc. **127**, 763–768 (2019).
21. A. Roggan, D. Schädel, U. Netz, J. P. Ritz, C. T. Germer, and G. Müller, "The effect of preparation technique on the optical parameters of biological tissue," Appl. Phys. B **69**, 445 (1999).
22. S. A. Prahl, M. J. C. Van Gemert, and A. J. Welch, "Determining the optical properties of turbid media by using the adding-doubling method," Appl. Opt. **32**, 559 (1993).
23. F. P. Bolin, L. E. Preuss, R. C. Taylor, and R. J. Ference, "Refractive index of some mammalian tissues using a fiber optic cladding method," Appl. Opt. **28**, 2297 (1989).
24. O. Hamdy, J. El-Azab, T. A. Al-Saeed, M. F. Hassan, and N. H. Solouma, "A method for medical diagnosis based on optical fluence rate distribution at tissue surface," Materials **10**, 1104 (2017).
25. R. Splinter, W. F. Cheong, M. J. C. van Gemert, and A. J. Welch, "*In vitro* optical properties of human and canine brain and urinary bladder tissues at 633 nm," Lasers Surg. Med. **9**, 37 (1989).
26. D. J. Maitland, J. T. Walsh, and J. B. Prystowsky, "Optical properties of human gallbladder tissue and bile," Appl. Opt. **32**, 586 (1993).
27. D. Zhu, Q. Luo, and J. Cen, "Effects of dehydration on the optical properties of *in vitro* porcine liver," Lasers Surg. Med. **33**, 226 (2003).
28. S. Rastegar and M. Motamedi, "A theoretical analysis of dynamic variation of temperature dependent optical properties in the response of laser irradiated tissue," Proc. SPIE **1202**, 253 (1990).
29. H. Ao, D. Xing, H. Wei, H. Gu, G. Wu, and J. Lu, "Thermal coagulation-induced changes of the optical properties of normal and adenomatous human colon tissues *in vitro* in the spectral range 400–1100 nm," Phys. Med. Biol. **53**, 2197 (2008).

30. L. Wang, S. L. Jacques, and L. Zheng, "Determination of fluence rate distribution in a multilayered skin tissue model by using Monte Carlo simulations," Comput. Methods Prog. Biomed. **47**, 131 (1995).
31. H. Arslan and B. Pehlivanoz, "Light dosimetry: effects of dehydration and thermal damage on the optical properties of the human aorta," Turk. J. Phys. **43**, 286 (2019).
32. I. F. Çilesiz and A. J. Welch, "Optical properties of normal and thermally coagulated chicken liver tissue measured ex-vivo with diffuse reflectance," Appl. Opt. **32**, 477 (1993).
33. M. Atif, S. Firdous, M. S. Mehmood, M. Y. Hamza, M. Imran, G. Hussain, and M. Ikram, "MCML—Monte Carlo modeling of light transport in multilayered tissues," Opt. Spectrosc. **110**, 313 (2011).